

Multimodal Safe Control for Human-Robot Interaction

Ravi Pandya, Tianhao Wei, Changliu Liu

Abstract—Generating safe behaviors for autonomous systems is important as they continue to be deployed in the real world, especially around people. In this work, we focus on developing a novel safe controller for systems where there are multiple sources of uncertainty. We formulate a novel multimodal safe control method, called the Multimodal Safe Set Algorithm (MMSSA) for the case where the agent has uncertainty over which discrete mode the system is in, and each mode itself contains additional uncertainty. To our knowledge, this is the first energy-function-based safe control method applied to systems with multimodal uncertainty. We apply our controller to a simulated human-robot interaction where the robot is uncertain of the human’s true intention and each potential intention has its own additional uncertainty associated with it, since the human is not a perfectly rational actor. We compare our proposed safe controller to existing safe control methods and find that it does not impede the system performance (i.e. efficiency) while also improving the safety of the system.

I. INTRODUCTION

Guaranteeing that autonomous systems can stay safe is becoming increasingly important as robots are being deployed in the real world. Such autonomous agents need to consider how to keep themselves safe (e.g. avoid collisions with objects) but also how to keep other agents safe. In particular, robots need to ensure that people working with and around them are also kept safe from harm. This means we need to design autonomous robots in a way that we know they will not put people in unsafe situations.

One well-known approach to this problem is to design a safe control law that guarantees that the the safe region of the state space is *forward invariant*, i.e. the system will not leave the safe region once it enters it. Additionally, many safe controllers are designed to guarantee *finite-time convergence* to the safe region if the system is in an unsafe state. Many safe control laws are designed by first writing down a scalar energy function which encodes the control objective of staying safe. The energy function is usually designed such that if the energy function is negative, the system is in a safe state. A safe control law can then be designed such that if the system is in an unsafe state, the energy function will decrease (i.e. the time derivative of the energy function is negative). Some examples of energy-function-based safe control are control barrier functions (CBFs) [1], sliding mode control [2] and the safe set algorithm (SSA) [3].

In this work, we focus on the application of safe control methods to human-robot interaction, so we need to additionally handle safe control under uncertainty since we can never perfectly predict how humans act. It has long been

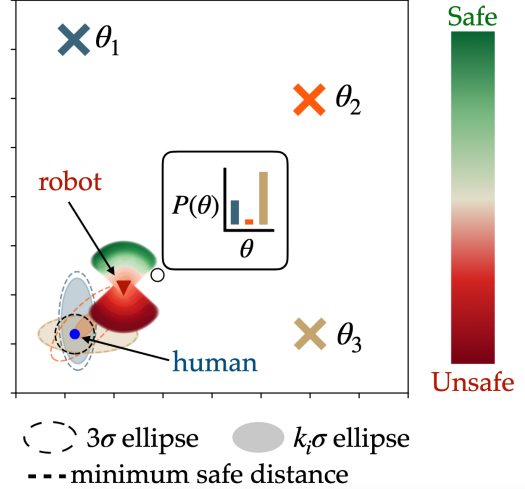


Fig. 1: Depiction of a multimodal human-robot system where the robot needs to stay safe with all potential goals θ_i the human might choose. The shaded region shows how safe potential future positions are, colored by the distance to the safe set of the corresponding control action.

known in other fields like cognitive science and behavioral economics that humans are not perfectly rational decision makers [4], [5], so it is better to model human behavior with probability distributions. Given a particular intention, the same person may not choose the same low-level actions to achieve their intention every time, so this is one layer of uncertainty the robot needs to deal with. On top of this, robots cannot explicitly know the intentions of people a priori, so robots need to infer their intentions, which adds an additional source of uncertainty.

As a result, we need new methods for guaranteeing safety under this kind of multimodal uncertainty. There is existing work on energy-function-based safe control under uncertainty [6], though it only considers unimodal uncertainty.

Our contributions in this work are the following:

- 1) A novel formulation of multimodal safe control for a robot interacting with people;
- 2) A derivation of a least-conservative safe control law for a dynamics model with multimodal uncertainty;
- 3) A comparison with existing safe control.

II. PROBLEM FORMULATION

A. Energy-Function-Based Safe Control

As previously mentioned, a popular approach for designing a safe control law is to construct a scalar energy function (or *safety index*) that indicates how safe the system state currently is. Concretely, the safety index $\phi : \mathcal{X} \rightarrow \mathbb{R}$

Authors are with Carnegie Mellon University, Pittsburgh, PA, USA {rapandya, twei2, cliu6}@andrew.cmu.edu

maps the state space \mathcal{X} to the reals. The function should be designed such that the system is safe if $\phi(x) \leq 0$. We want to design a safe control law that decreases $\phi(x)$ when the system is unsafe, and even in safe situations, $\phi(x)$ should not increase too quickly. This means our safety constraint becomes an inequality constraint on $\dot{\phi}(x)$:

$$\dot{\phi}(x) = \nabla_x \phi^T(x) \dot{x} \leq \eta(\phi) \quad (1)$$

where $\eta(\phi)$ is our margin for safety, or the maximum rate of increase of $\phi(x)$. For ease of notation going forward, we will write $\nabla_x \phi^T(x)$ simply as $\nabla_x \phi^T$.

The general problem of designing $\phi(x)$ for an arbitrary system is challenging, but is not the focus of this work. There is a breadth of existing literature on writing or synthesizing safety indices [3], [7], [8]. Thus we assume that we are given a safety index ϕ for our system that we must design a safe control law around.

B. Multimodal Dynamical System

We assume the system is in control-affine form¹

$$\dot{x} = f(x, \theta) + g(x)u, \quad (2)$$

where θ follows a discrete probability distribution $\theta \sim \{\theta_1, \theta_2 \dots \theta_N\}$ and $f(x, \theta_i) \sim \mathcal{N}(m(x, \theta_i), \Sigma(x, \theta_i))$. In this work, we focus on additive multimodal uncertainty in f and not multiplicative multimodal uncertainty in g . Since the robot cannot exert direct control over the human, it is natural to represent the human's uncertain dynamics through uncertainty in f (Sec. IV-A).

We are given a safety index ϕ , so following from (1):

$$\nabla_x \phi^T(f(x, \theta) + g(x)u) \leq \eta(\phi) \quad (3)$$

$$\nabla_x \phi^T f(x, \theta) + \nabla_x \phi^T(x)g(x)u \leq \eta(\phi) \quad (4)$$

$$\underbrace{\nabla_x \phi^T g(x)}_{L(x)} u \leq \underbrace{\eta(\phi) - \nabla_x \phi^T f(x, \theta)}_{S(x)}. \quad (5)$$

Ultimately, this gives us a half-space constraint on the set of control inputs, so our set of safe controls is defined as $\mathcal{U}^S(x) = \{u \mid L(x)u \leq S(x)\}$.

Since we are dealing with a stochastic system, the robust safe control should be chosen such that we have a high probability of satisfying the safety constraint

$$P[\dot{\phi} \leq \eta(\phi)] \geq 1 - \epsilon \quad (6)$$

where $1 - \epsilon$ is our desired probability of safety. Like in (5), we can substitute the system dynamics to equivalently get:

$$P[\nabla_x \phi^T g(x)u \leq \eta(\phi) - \nabla_x \phi^T f(x, \theta)] \geq 1 - \epsilon. \quad (7)$$

III. MULTIMODAL SAFE SET ALGORITHM

A. Naive Multimodal Safe Control (N-MMSSA)

Since we are working with normally distributed $f(x, \theta_i)$, the original probabilistic constraint will be satisfied if

$$\sum_i P(\theta_i) \Gamma(k_i) \geq 1 - \epsilon \quad (8)$$

¹An arbitrary control system can be transformed to the control-affine form through dynamic extension.

where Γ is the normalized CDF of the Gaussian probability distribution such that $\Gamma(0) = \frac{1}{2}$ and k_i is the number of standard deviations satisfied for mode i since we need to bound the tail of the Gaussian distribution. For example, if the system is unimodal and $\epsilon = 0.003$, then we can choose $k = 3$ to satisfy the probabilistic constraint because $\Gamma(3) = 0.997$, meaning 99.7% of the probability mass is within a 3σ bound.

Let us define $\delta(x, \theta) = f(x, \theta) - m(x, \theta)$ as the difference between the true (noisy) dynamics and the mean dynamics. Since $g(x)$ is assumed to be deterministic, the terms cancel out here. Now we can use this to define the 1σ worst case value of $\nabla_x \phi^T \delta(x, \theta)$, which represents the maximum difference between the control constraint $S(x)$ that would come from the mean dynamics and that would come from the true noisy dynamics. This difference, which we call $\gamma(x, \theta)$ is what we want our controller to be robust to:

$$\gamma(x, \theta) = \max_{\delta^T(x, \theta) \Sigma^{-1}(x, \theta) \delta(x, \theta) \leq 1} \nabla_x \phi^T \delta(x, \theta). \quad (9)$$

Then the $k\sigma$ worst case situation is $k\gamma(x, \theta)$. This means $k\gamma(x, \theta)$ is the maximum value that $\nabla_x \phi^T f(x, \theta)$ will deviate from $\nabla_x \phi^T m(x, \theta)$. Then we can compute our robust control constraint by substituting $\nabla_x \phi^T m(x, \theta) + k\gamma(x, \theta)$ in place of $\nabla_x \phi^T f(x, \theta)$ back in to the original constraint (7) (which was not computable). We then get one constraint per mode that we can directly compute:

$$\nabla_x \phi g(x)u \leq \eta(\phi) - \nabla_x \phi m(x, \theta_i) - k_i \gamma(x, \theta_i), \quad (10) \\ \forall i = \{1, \dots, N\}$$

where k_i is the desired level to stay safe with respect to for mode i . To satisfy the probabilistic constraint (8), we need a way to pick the $k\sigma$ bound for each mode. One easy way to guarantee this constraint is satisfied is to pick a fixed value k for all k_i such that $\Gamma(k) \geq 1 - \epsilon$. For example, our experiments use $\epsilon = 0.003$, which gives us that any $k \geq 3$ will allow us to satisfy our constraint. We refer to this method as the Naive Multimodal Safe Set Algorithm (N-MMSSA). The final constraints for the naive version are then:

$$\underbrace{\nabla_x \phi^T g(x)}_{L(x)} u \leq \underbrace{\eta(\phi) - \nabla_x \phi^T m(x, \theta_i) - k\gamma(x, \theta_i)}_{S_i(x)}, \quad (11) \\ \forall i = \{1, \dots, N\}.$$

where k is chosen such that $\Gamma(k) \geq 1 - \epsilon$. These constraints define the set of safe controls $\mathcal{U}^S(x) = \{u \mid L(x)u \leq S_i(x), \forall i\}$. Since all the constraints are parallel in the control space (since $L(x)$ does not depend on θ), we can take the most conservative constraint to define the safe set of controls:

$$\mathcal{U}^S = \{u \mid L(x)u \leq S^*(x)\} \\ S^*(x) = \min_i S_i(x) \quad (12)$$

The safe control input will be determined by projecting a reference control u_{ref} to the set of safe controls \mathcal{U}^S . Since $L(x)u \leq S^*(x)$ is a linear constraint, this can be formulated

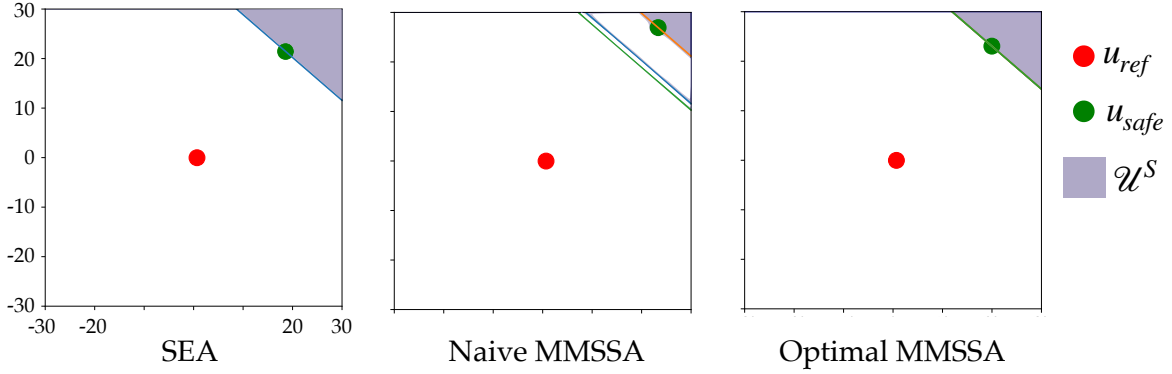


Fig. 2: The control constraints from each safe control method at the same system state.

as a quadratic program:

$$u_{safe} = \operatorname{argmin}_{u \in \mathcal{U}^S} \|u - u_{ref}\|_2^2. \quad (13)$$

Following the original Safe Set Algorithm [3], the safety controller should only be active when necessary:

$$u = \begin{cases} u_{safe}, & \text{if } \phi \geq 0 \\ u_{ref}, & \text{otherwise} \end{cases} \quad (14)$$

Though this method will satisfy the probabilistic safety constraint, it may be overly conservative, since it stays safe with respect to a fixed bound per mode θ_i , even if the probability $P(\theta_i)$ that the system is in that mode is arbitrarily low. Notice that in Fig. 2, this controller picks the most conservative control constraint, so we look for a way to more intelligently choose k for each mode.

B. Optimal Multimodal Safe Control (O-MMSSA)

Instead of naively choosing a fixed $k\sigma$ bound for all modes, the least-conservative safe control will try to distribute the constraints equally among all modes. We will define $\mu(x, \theta_i, k_i) = \nabla_x \phi^T m(x, \theta_i) + k_i \gamma(x, \theta_i)$, so we can choose the desired $\mathbf{k} = [k_1, \dots, k_N]^T$ by solving the following constrained optimization:

$$\begin{aligned} \min_{\mathbf{k}} & \left\{ \max_{i,j} \{ \mu(x, \theta_i, k_i) - \mu(x, \theta_j, k_j) \} + \|\mathbf{k}\|_2 \right\} \\ \text{s.t.} & \sum_i P(\theta_i) \Gamma(k_i) \geq 1 - \epsilon. \end{aligned} \quad (15)$$

This optimization is trying to find the smallest $k\sigma$ bound for each mode that results in the smallest possible difference between all pairs of control constraints while satisfying the probabilistic constraint. After optimizing for all k_i 's, we can then directly compute the safety constraints shown in (10). We can see in Fig. 2 that all three resulting control constraints are essentially overlapping. In practice, the inner optimization can be computed exactly since it is over discrete variables, and the outer optimization is solved with Sequential Least Squares Programming (SLSQP) [9]. This controller resulting from this method of optimally selecting the $k\sigma$ bound per mode is called the Optimal Multimodal Safe Set Algorithm (**O-MMSSA**). The final control input can be computed using the same method as in N-MMSSA, shown in (14).

C. Comparison with Unimodal Safe Control (SEA)

As a baseline comparison, we use a controller from prior work that does safe control under Gaussian uncertainty [6], called SEA (Safe Exploration Algorithm). In the original paper, the robot considers only the most-likely mode $\theta' = \operatorname{argmax}_{\theta} P(\theta)$ of the human. Just as in the original paper, the robot considers staying safe with respect to a 3σ bound on the uncertainty of the human's dynamics to satisfy the desired level of safety (6).

We note that this approach is not guaranteed to be safe with respect to the multimodal system, since this *unimodal* approach essentially takes $k_i = 3$ for one mode and $k_i = 0$ for all other modes. In a simple bimodal system where $P(\theta_1) = P(\theta_2) = 0.5$, it's easy to see that simply setting $k_1 = 3, k_2 = 0$ will not satisfy (8). Intuitively, we can see in Fig. 2 that SEA picks the least conservative constraint in this case, which may not be safe if the true system is in a different mode.

We additionally note that the original paper that proposes SEA modifies the safety index ϕ in order to stay safe with respect to a 3σ bound, but we instead include it in the control constraint for a more fair comparison between the methods discussed here (so all methods use the same safety index). This means the robot's safe control imposes the following linear constraint on the control space:

$$\nabla_x \phi g(x) u \leq \eta(\phi) - \nabla_x \phi m(x, \theta') - k' \gamma(x, \theta') \quad (16)$$

where $\Gamma(k') \geq 1 - \epsilon$. Once again, the final control input can be computed by solving the same QP as in N-MMSSA and O-MMSSA (14).

IV. APPLICATION TO HUMAN-ROBOT SYSTEM

A. Dynamics

Though the formulation itself is applicable to general multimodal control-affine systems, we focus on the case of human-robot interaction, since this is a realistic real-world instantiation of the multimodal control problem. Specifically, we consider \dot{x} to be the joint human-robot system dynamics:

$$\begin{bmatrix} \dot{x}_R \\ \dot{x}_H \end{bmatrix} = \begin{bmatrix} f_R(x_R) \\ h(x_H, x_R, \theta) \end{bmatrix} + \begin{bmatrix} g_R(x_R) \\ 0 \end{bmatrix} u_R. \quad (17)$$

where $x_H \in \mathbb{R}^{n_H}$ and $x_R \in \mathbb{R}^{n_R}$ are the states of the human and robot respectively, $u_R \in \mathbb{R}^{m_R}$ is the robot's

control input, $f_R(x_R) : \mathbb{R}^{n_R} \rightarrow \mathbb{R}^{n_R}$ and $g_R(x_R) : \mathbb{R}^{n_R} \rightarrow \mathbb{R}^{n_R \times m_R}$ define the robot's dynamics and $h(x_H, x_R, \theta) : \mathbb{R}^{n_H} \times \mathbb{R}^{n_R} \rightarrow \mathbb{R}^{n_H}$ defines the human's dynamics. Since the robot's dynamics are deterministic, we have

$$m(x, \theta_i) = \begin{bmatrix} f_R(x_R) \\ m_H(x_H, x_R, \theta) \end{bmatrix} \quad (18)$$

$$\Sigma(x, \theta_i) = \begin{bmatrix} 0 & 0 \\ 0 & \Sigma_H(x, \theta_i) \end{bmatrix} \quad (19)$$

where $\Sigma_H(x, \theta)$ defines the covariance matrix of the human's dynamics $h(x_H, x_R, \theta) \sim \mathcal{N}(m_H(x_H, x_R, \theta), \Sigma_H(x, \theta))$. Note that the robot has no direct control over the human. In the human-robot system, each θ_i corresponds to a potential intention of the human (for example, different goal locations to reach). The human's true intention θ^* is unknown to the robot, so the robot needs to estimate it online.

B. Human Intent Inference

To estimate the human's intention, the robot keeps a belief $b_R^t = [P(\theta_1), \dots, P(\theta_N)]$ over the human's intention, which represents the probability that $\theta_i = \theta^*$.

Following prior work, the robot assumes a Boltzmann-rational model of the human's behavior, a model commonly used in fields related to human decision making [10], [11], especially human-robot interaction [12], [13]. Specifically, this means the human is exponentially more likely to choose an action if it has a higher Q-value (where the Q-value is the action-value function in the human's Markov Decision Process):

$$p(u_H^t | x_H^t, x_R^t; \theta) = \frac{e^{\beta_R Q_H(x_H^t, x_R^t, u_H^t; \theta)}}{\int_{u_H'} e^{\beta_R Q_H(x_H^t, x_R^t, u_H'; \theta)}}, \quad (20)$$

where β_R is the rationality coefficient (sometimes called the "inverse temperature" parameter or the "model confidence").

In general, this quantity can be difficult to compute, especially computing the integral in the denominator without discretizing the action space. While this is a common approach, we instead follow prior work [14] to utilize the known form of the human's control input to compute an exact form for this probability (Sec. V-B).

The robot uses this likelihood function to update b_R^t at some discrete time interval using Bayes' Rule:

$$\begin{aligned} b_R^t(\theta_i) &= p(\theta_i | x_H^{0:t}, x_R^{0:t}, u_H^{0:t}) \\ &= \frac{p(u_H^t | x_H^t, x_R^t; \theta_i) p(\theta_i | x_H^{0:t-1}, x_R^{0:t-1}, u_H^{0:t-1})}{\sum_{\theta'} p(u_H^t | x_H^t, x_R^t; \theta') p(\theta' | x_H^{0:t-1}, x_R^{0:t-1}, u_H^{0:t-1})} \end{aligned} \quad (21)$$

V. SIMULATION SETUP

A. Simulated Dynamics Models

The robot has deterministic unicycle dynamics $\dot{x}_R = f_R(x_R) + g_R(x_R)u_R$:

$$\dot{x}_R = \begin{bmatrix} \dot{x} \\ \dot{y} \\ \dot{v}_R \\ \dot{\psi}_R \end{bmatrix} = \begin{bmatrix} v_R \cos \psi_R \\ v_R \sin \psi_R \\ 0 \\ 0 \end{bmatrix} + \begin{bmatrix} 0 & 0 \\ 0 & 0 \\ 1 & 0 \\ 0 & 1 \end{bmatrix} u_R \quad (22)$$

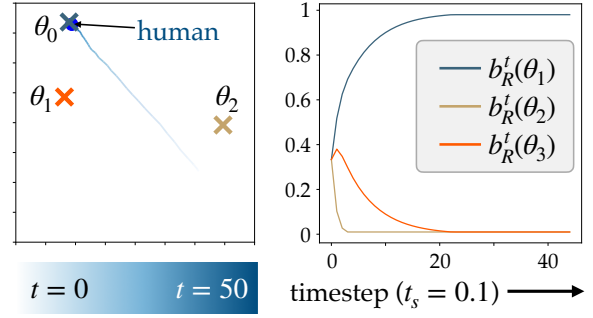


Fig. 3: Bayesian inference of the simulated human's goal

where the robot's control input is the acceleration and steering angle $u_R = [\dot{v}_R, \dot{\psi}_R]^T$.

The human has noisy double-integrator LTI dynamics $\dot{x}_H = Ax_H + Bu_H + w(t)$:

$$\dot{x}_H = \begin{bmatrix} \dot{h}_x \\ \dot{v}_x \\ \dot{h}_y \\ \dot{v}_y \end{bmatrix} = \begin{bmatrix} 0 & 1 & 0 & 0 \\ 0 & 0 & 0 & 0 \\ 0 & 0 & 0 & 1 \\ 0 & 0 & 0 & 0 \end{bmatrix} x_H + \begin{bmatrix} 0 & 0 \\ 1 & 0 \\ 0 & 0 \\ 0 & 1 \end{bmatrix} u_H + w(t), \quad (23)$$

where $w(t) \sim \mathcal{N}(0, \Sigma)$. $m_H(x_H, x_R, \theta)$ is the dynamics without noise: $m_H(x_H, x_R, \theta) = Ax_H + Bu_H$. We assume the human's control has the following form:

$$u_H = -K(x_H - \theta) + \frac{\gamma}{d^2}(C_H x_H - C_R x_R) \quad (24)$$

where C_H and C_R are constant matrices that select the x and y positions of the respective agent's state, $d = \|C_R x_R - C_H x_H\|_2$ and $\gamma \in \mathbb{R}$ determines how strongly the human is repelled from the robot. Specifically,

$$C_H = \begin{bmatrix} 1 & 0 & 0 & 0 \\ 0 & 0 & 1 & 0 \end{bmatrix} \quad (25)$$

$$C_R = \begin{bmatrix} 1 & 0 & 0 & 0 \\ 0 & 1 & 0 & 0 \end{bmatrix}. \quad (26)$$

The gain K is the solution to the infinite-horizon linear-quadratic regulator (LQR) problem with diagonal weight matrices Q, R that minimizes

$$\int_0^\infty ((x_H - \theta)^T Q (x_H - \theta) + u_H^T R u_H) dt. \quad (27)$$

B. Goal Inference on Simulated Human

In the simulated system, each θ_i is a potential goal location that the human is moving towards. Since the human's control input is primarily governed by this goal-reaching controller computed via LQR, we use the LQR cost to define the robot's inference. In order to write down a Q-value function in closed form, the robot treats the effect of its own state on the human's control as noise in the human's decision making². Drawing on prior work [14], we consider the human's reward function to be the negative instantaneous LQR cost:

$$r_H(x_H, u_H; \theta) = -(x_H - \theta)^T Q (x_H - \theta) - u_H^T R u_H. \quad (28)$$

²This could alternatively be viewed as the robot only having knowledge of the human's goal-seeking control, so it has no choice but to include other influences on the human's control as unobserved noise.

Since there is no dependence on x_R , we have dropped it as an argument. The Q-value (or action-value) function is only well-defined in discrete time³, so to properly do inference on the human's goal, we consider the equivalent discrete-time dynamics model of the human (\tilde{A}, \tilde{B}). In this case, we know that the action-value function is the negative infinite-time optimal cost-to-go for LQR after the human takes u_H :

$$Q_H(x_H, u_H; \theta) = r(x_H, u_H; \theta) - (x' - \theta)^T P (x' - \theta) \quad (29)$$

where $x' = \tilde{A}x_H + \tilde{B}u_H$ and P is the solution to the discrete-time algebraic Riccati equation (DARE):

$$P = \tilde{A}^T P \tilde{A} - \tilde{A}^T P \tilde{B} (R + \tilde{B}^T P \tilde{B})^{-1} \tilde{B}^T P \tilde{A} + Q. \quad (30)$$

From the derivation in [14], we can compute an explicit form of the denominator of $p(u_H^t | x_H^t; \theta)$ because it takes the form of a Gaussian integral:

$$\begin{aligned} & \int e^{\beta_R Q_H(x_H, u_H; \theta)} \\ &= e^{-\beta_R (x_H - \theta)^T P (x_H - \theta)} \sqrt{\frac{(2\pi)^m}{\det(2\beta_R R + 2\beta_R \tilde{B}^T P \tilde{B})}}. \end{aligned} \quad (31)$$

The robot then uses this computed likelihood function to update its belief using Bayes Rule (21) given a new observation (x_H^t, u_H^t) .

Rolling this inference out on the simulated system, we can see in Fig. 3 that the robot's belief correctly converges to the human's intended goal θ_0 after about 25 observations. We can also see that the probability of θ_1 initially increases, which makes sense, since the robot observes the human moving in the direction of both θ_0 and θ_1 . Similarly, the probability of θ_2 immediately decreases since the human is moving away from that goal.

C. Nominal Robot Control

The robot's nominal control $u_{ref} = [\dot{v}_R, \dot{\psi}_R]^T$ drives it towards its own goal state $[g_x, g_y]$ which defines an (x, y) position. Let $\delta_x = (r_x - g_x)$ and $\delta_y = (r_y - g_y)$, then:

$$\dot{v}_R = -[\delta_x \cos \psi_R + \delta_y \sin \psi_R] - k_v v_R \quad (32)$$

$$\dot{\psi}_R = k_\psi \left[\arctan \frac{\delta_y}{\delta_x} - \psi_R \right] \quad (33)$$

where $k_v, k_\psi \in \mathbb{R}^+$ are constants. The controller is designed according to the Lyapunov function $V = \delta_x^2 + \delta_y^2 + v_R^2$.

D. Safe Control

The safety index is designed as $\phi = d_{min}^2 - d^2 - k_\phi \dot{d}$ where d is the relative Cartesian distance between the agents and $k_\phi \in \mathbb{R}^+$ is a constant coefficient. In order to compute the

³In continuous time, the human's action shows up as the time derivative of the optimal cost-to-go, but for simplicity, we build on existing discrete-time Bayesian inference approaches.

	SEA	N-MMSSA	O-MMSSA
# safety violations per rollout	0.11	0.07	0.02
# goals reached per rollout	3.24	3.31	3.4
control set size ($rad \cdot m/s^2$)	195.9	122.7	160.5

TABLE I: Average safety and efficiency metrics.

control input for all methods, we need to compute $\nabla_{x_H} \phi$ and $\nabla_{x_R} \phi$. The derivations are left out for space, but we have:

$$\begin{aligned} & \nabla_{x_H} \phi = \\ & 2d_p^T C_H + k_\phi \left[\frac{1}{d} d_v^T C_H + \frac{1}{d} d_p^T B^T - \frac{1}{d^3} d_p^T d_v d_p^T C_H \right] \end{aligned} \quad (34)$$

$$\begin{aligned} & \nabla_{x_R} \phi = \\ & -2d_p^T C_R - k_\phi \left[\frac{1}{d} d_v^T C_R + \frac{1}{d} d_p^T \mathcal{V} - \frac{1}{d^3} d_p^T d_v d_p^T C_R \right] \end{aligned} \quad (35)$$

where $d_p = C_R x_R - C_H x_H$ so that $d = \|d_p\|$, $d_v = \dot{d}_p$ and

$$\mathcal{V} := \begin{bmatrix} 0 & 0 & \cos \theta_R & -v_R \sin \theta_R \\ 0 & 0 & \sin \theta_R & v_R \cos \theta_R \end{bmatrix}. \quad (36)$$

VI. SIMULATION RESULTS

We compare the performance of our proposed controller O-MMSSA (Sec. III-B) against the two baselines: N-MMSSA (Sec. III-A) and SEA (Sec. III-C). We are interested in two metrics: the *safety* and *efficiency* of each controller. In our evaluations, we set $\epsilon = 0.003$ and $d_{min} = 1m$. The agents' dynamics are implemented in continuous-time and integrated forward with a Runge-Kutta method (RK4) with a sampling time $t_s = 0.1$ seconds. The time horizon for each trajectory is $25s$. Each simulation consists of a randomly sampled initial condition for the human and robot's positions as well as the set of goals $\{\theta_1, \dots, \theta_4\}$.

We measure safety by looking at the number of timesteps that the robot violated the minimum distance constraint. We measure efficiency by looking at two things: 1) the number of goals reached by the robot in the time horizon and 2) the volume of the safe set of controls (assuming $\|u_R\|_\infty \leq 30$).

We run 100 initial conditions per controller and average the results across all (note that all three controllers are run with the same set of initial conditions for a fair comparison). The results are shown in Table I. We can see that the O-MMSSA controller reaches the highest number of goals on average, while N-MMSSA and SEA let the robot reach fewer goals. This is a good sign, since it means that our proposed controller allows the robot to be more efficient at completing its task than other baseline controllers. We also see that SEA has more safety violations on average than either O-MMSSA or N-MMSSA. This tells us that while SEA may be relatively efficient, using the unimodal safe control approach on a multimodal system may leave the system in unsafe states.

To get a sense of why SEA may leave the system in unsafe states, we can look at Fig. 4. Here, we see that the most likely goal of the human is θ_1 , even when the human starts moving

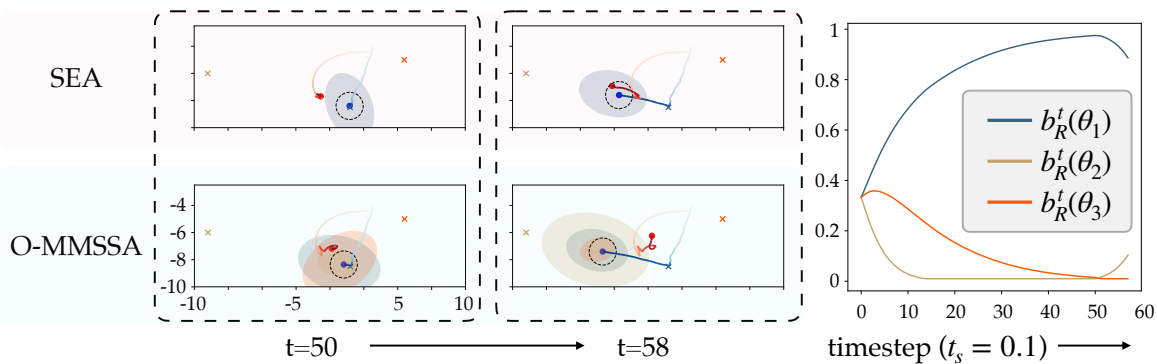


Fig. 4: An example of unimodal safe control (Sec. III-C) violating the minimum safe distance from the human while the proposed multimodal safe controller (Sec. III-B) does not.

toward θ_2 , since the robot’s intent inference takes multiple observations to change drastically⁴. As a result, SEA does not prepare for the possibility that the human’s true goal may be different, resulting in the robot being in a state where a safety violation is inevitable, and happens at $t = 58$. Meanwhile, O-MMSSA accounts for this possibility at $t = 50$ and is already out of the way of the human by $t = 58$.

Finally, we also see in Table I that SEA keeps the safe set of controls the largest, followed by O-MMSSA then N-MMSSA. Even though SEA keeps this set the largest, it results in the most safety violations, which tells us that often times the safety constraints are inaccurate. Meanwhile, O-MMSSA keeps the safe set of controls larger than N-MMSSA does, which means it is less conservative while staying safe.

VII. CONCLUSION AND FUTURE WORK

We presented a novel formulation of safe control for systems with multimodal uncertainty where the system may be in one of multiple discrete modes and each mode has its own associated dynamics noise. We derived a least-restrictive controller (O-MMSSA) that balances the resulting control constraints from each mode to keep the safe set of controls as large as possible. We evaluated our proposed controller against a naive multimodal safe control baseline (N-MMSSA) and a unimodal safe controller (SEA) based on prior work. When evaluating on a simulated human-robot system, we found that our proposed controller keeps the human-robot system more safe than the unimodal baseline and keeps the set of safe controls larger than the naive multimodal baseline. This tells us that our proposed controller is helpful for improving both the safety and efficiency of human-robot interactions.

Future work may additionally study how to deal with multiplicative uncertainty in the system (i.e. $g(x)$ has multimodal uncertainty), as well as test how these controllers perform on physical robots interacting with real humans.

ACKNOWLEDGMENTS

This material is based upon work supported by the National Science Foundation Graduate Research Fellowship

⁴This is desired behavior in real HRI systems. Since humans are noisy actors, we don’t want to infer the human’s intent from just one action.

under Grant No. DGE1745016 and DGE2140739 and additionally under Grant No. 2144489. Any opinions, findings, and conclusions or recommendations expressed in this material are those of the authors and do not necessarily reflect the views of the National Science Foundation. This work is additionally supported by the Manufacturing Futures Institute, Carnegie Mellon University, through a grant from the Richard King Mellon Foundation.

REFERENCES

- [1] A. D. Ames, S. Coogan, M. Egerstedt, G. Notomista, K. Sreenath, and P. Tabuada, “Control barrier functions: Theory and applications,” in *2019 18th European control conference (ECC)*. IEEE, 2019, pp. 3420–3431.
- [2] M. A. Gomez, C. D. Cruz-Ancona, and L. Fridman, “Safe sliding mode control,” in *2022 19th International Conference on Electrical Engineering, Computing Science and Automatic Control (CCE)*. IEEE, 2022, pp. 1–6.
- [3] C. Liu and M. Tomizuka, “Control in a safe set: Addressing safety in human-robot interactions,” in *Dynamic Systems and Control Conference*, vol. 46209. American Society of Mechanical Engineers, 2014, p. V003T42A003.
- [4] H. A. Simon, *Models of bounded rationality: Empirically grounded economic reason*. MIT press, 1997, vol. 3.
- [5] J. Conlisk, “Why bounded rationality?” *Journal of economic literature*, vol. 34, no. 2, pp. 669–700, 1996.
- [6] C. Liu and M. Tomizuka, “Safe exploration: Addressing various uncertainty levels in human robot interactions,” in *2015 American Control Conference (ACC)*. IEEE, 2015, pp. 465–470.
- [7] A. Clark, “Verification and synthesis of control barrier functions,” in *2021 60th IEEE Conference on Decision and Control (CDC)*. IEEE, 2021, pp. 6105–6112.
- [8] W. Zhao, T. He, T. Wei, S. Liu, and C. Liu, “Safety index synthesis via sum-of-squares programming,” in *2023 American Control Conference (ACC)*. IEEE, 2023, pp. 732–737.
- [9] D. Kraft, “A software package for sequential quadratic programming,” *Forschungsbericht- Deutsche Forschungs- und Versuchsanstalt für Luft- und Raumfahrt*, 1988.
- [10] D. McFadden *et al.*, “Conditional logit analysis of qualitative choice behavior,” *Frontiers in Econometrics*, 1973.
- [11] D. McFadden, “The measurement of urban travel demand,” *Journal of public economics*, vol. 3, no. 4, pp. 303–328, 1974.
- [12] C. L. Baker, J. B. Tenenbaum, and R. R. Saxe, “Goal inference as inverse planning,” in *Proceedings of the Annual Meeting of the Cognitive Science Society*, vol. 29, no. 29, 2007.
- [13] S. Levine and V. Koltun, “Continuous inverse optimal control with locally optimal examples,” *arXiv preprint arXiv:1206.4617*, 2012.
- [14] R. Tian, M. Tomizuka, A. D. Dragan, and A. Bajcsy, “Towards modeling and influencing the dynamics of human learning,” in *Proceedings of the 2023 ACM/IEEE International Conference on Human-Robot Interaction*, 2023, pp. 350–358.